Supporting Information

Lanz et al. 10.1073/pnas.1302569110

SI Materials and Methods

Microarray Analysis. After mouse brain microvascular endothelial cells (MBMEC) culture for 1 wk, one half had been treated for 24 h with tumor necrosis factor (TNF)-α 500 U/mL and interferon (IFN)-γ 500 U/mL ("inflamed" setting) whereas the other half had been left "naïve." For the last 8 h of culture, half of each group had been treated with LY-317615 to obtain the following conditions: (*i*) naïve, DMSO control; (*ii*) naïve with 5 μM LY-317615; (*iii*) inflamed setting, LY-317615 treatment; and (*iv*) inflamed setting with 5 μM LY-317615. Samples were prepared as biological triplicates. Total RNA from MBMEC was isolated using the TRIzol Plus (Invitrogen) RNA purification method according to the manufacturer's instructions. The quality and concentration of total RNA was checked by gel analysis using the total RNA Pico chip assay on an Agilent 2100 Bioanalyzer (Agilent Technologies GmbH). Hybridization to microarrays (Mouse WG-6 v2.0 Expression BeadChip; Illumina Inc.) was performed according to the manufacturer's recommended experimental protocol. Microarray scanning was done using an iScan array scanner (Illumina Inc.). Data extraction was done for all beads individually, and outliers were removed when the absolute difference to the median was greater than 2.5 times. All remaining bead-level data points were then quantile-normalized (1). Differentially expressed genes were identified by using Student *t* test on log-transformed data (*P* values were two-sided). Benjamini–Hochberg correction was used to control the false discovery rate (FDR). Hypergeometric enrichment analysis of Kyoto Encyclopedia of Genes and Genomes (KEGG) pathways among the differentially expressed genes (FDR < 0.05 and fold change > 1.2) between LY-317615–treated and control-treated endothelial cells was performed using Graphite Web with Benjamini–Hochberg correction (2).

Phospho-Kinase Antibody Array. After 1 wk of culture, MBMEC, as well as human umbilical vein endothelial cells (HUVEC) (PromoCell), were stimulated with 1 μM LY-317615 for 8 h. The human phospho-kinase antibody array was purchased from R&D and performed with protein lysates of the two cell lines according to the manufacturer's instructions. The manufacturer had assured that 15 of the 45 included antibody sets had been tested to cross-react with mouse proteins [p38alpha, c-Jun N-terminal kinases (JNK) pan, glycogen synthase kinase (GSK)-3 alpha/beta, mitogen and stress activated protein kinase (MSK) 1/2, 5′ AMP-activated protein kinase (AMPK)alpha1, Akt (S473), cAMP response element-binding protein (CREB), beta-Catenin, p70S6K (T421/S424), c-Jun, signal transducer and activator of transcription (STAT)5a, p70S6K (T389), ribosomal s6 kinase (RSK) 1/2/3, STAT3, and STAT5 a/b]. Another set of 5 antibodies [extracellular-signal regulated kinase (ERK)1/2, target of rapamycin (TOR), Src, Fyn, and focal adhesion kinase (FAK)] are putatively targeting their corresponding murine target proteins. Chemoluminescence was detected using an Agfa Classic E.O.S. developer with exposure times between 30 s and 30 min. Distinct detection of phosphorylated GSK3β was performed by Western blot analysis as described above and analyzed the same way. Scanned images were analyzed using Fiji software (3). Each signal was manually selected, and integrated density was measured as average gray value per pixel. Before statistical analysis, background subtraction was performed.

Adoptive Transfer. For induction of EAE by adoptive transfer of leukocytes, mice were immunized as described above. On day 9 after immunization, thus before onset of EAE symptoms, mice were killed, lymph nodes and spleens were mechanically disrupted, and cells were seeded in an upright cell-culture flask at a concentration of 7.5×10^6 cells per mL in enriched RPMI 1640 (supplemented with 10% (vol/vol) FBS, 100 U/mL penicillin, 0.1 mg/mL streptomycin, 1 mM Sodium Pyruvate (all from PAA), 0.1 mM nonessential amino acids (Lonza), 25 mM Hepes (Sigma), and 2 mM L-glutamine (Gibco/Invitrogen) containing $MOG_{35–55}$ 10 μg/mL After 3 d, cells were washed twice with PBS and injected i.p. into naïve SJL mice. Daily LY-317615 treatment of the recipient mice had started 3 d before the injection.

Immunohistochemistry. Mice were anesthetized by i.p. injection of 100 mg/kg ketamin and 20 mg/kg xylazin and then perfused with 50 mL of PBS by heart puncture. Brains and spinal cords were taken out and fixed in 4% (vol/vol) paraformaldehyde for 24 h and then transferred into 30% (wt/vol) sucrose for further storage. For detection of Evans Blue staining, macroscopic pictures were taken from spinal cords. For hematoxylin/eosin (H&E) and luxol-PAS staining, tissues were embedded in paraffin blocks and cut into 10-μm sections. Stainings were performed according to standard protocols. For immunohistochemistry of claudin 5, CD31, and CD3, spinal cords were shock-frozen in liquid nitrogen after perfusion. Tissue was cut into 30-μm slices (for claudin 5 and CD31) and into 10-μm slices (for CD3) using a cryomicrotome (Leica). Before staining, slices were fixed with Acetone for 10 min at −20 °C and then stained with the primary antibodies rat anti-mouse CD31 (BD Pharmingen), rabbit anti-claudin 5 (Invitrogen), and rabbit anti-CD3 (DAKO) according to standard protocols. Microscopy images were taken using an NiE inverted automated microscope and an A1R confocal microscope (Nikon). Statistical evaluation of infiltrating immune cells was obtained from H&E stainings by manually counting lesions of infiltrating cells. Demyelination was evaluated by manually counting demyelinated areas in luxol-PAS–stained spinal-cord slides, correlating it to the following score: 0.5, single demyelinated spot; 1, several spots; 2, confluent sites of demyelination; 3, demyelination of one half of the spinal cord; and 4, demyelination of more than half of the spinal cord. For statistical evaluation of CD3 lesion morphology, lesions larger than 10 cells were counted per cord section and were clustered into two groups: spread (lesion in which T cells have no connection to each other or to a vessel wall and were dispersed into the tissue) and confined (more than 70% of stained cells were stuck in one circumscribed vessel and a clear border of the lesions was easily visible). Morphological analyses and manual counting were carried out by a blinded investigator. All statistical evaluations were carried out in multiple slides of multiple animals as indicated in the corresponding figure legend.

Intracellular Detection of Cytokines by Flow Cytometry. For flow cytometric intracellular detection of cytokines, LY-317615 treatment started on the day of immunization. Lymph nodes were harvested 9 d after immunization and mechanically singularized as described above. Then 10^6 cells per well were seeded for 5 h in 24-well plates (TPP) in enriched RPMI with 20 ng/mL PMA, 1 μg/mL ionomycin, and 5 μg/mL brefeldin A (Sigma). Cells were stained for CD4 (BioLegend) and then permeabilized with cytofix/cytoperm solutions (BD Bioscience) and stained for IFN-γ, IL-17, and FoxP3 (ebioscience) according to standard protocols.

Western Blot Analysis of GSK3β and pGSK3β. Protein was isolated from in vitro $PLP_{139–151}$-restimulated T cells (as described above) or primary cultured MBMEC using standard buffers. Western blot analysis was carried out with rabbit anti-human/mouse GSK3β and rabbit anti-human/mouse pGSK3β (Cell Signaling) using standard protocols.

Detection of the Chemokines MCP-1 and IP-10. A fluorescent bead immunoassay (FlowCytomix; Bender MedSystems) was used to quantify the production of the chemokines MCP-1 and IP-10 by MBMEC according to the manufacturer's instructions. MBMEC had been treated with 5 μM LY-317615 for 18 h. Supernatants were analyzed for the designated chemokines by flow cytometry.

Real-Time PCR. RNA was isolated from MBMECs following standard procedures. cDNA synthesis was performed using a standard protocol with random hexamer primers (Applied Biosystems), and real-time PCR was run with Taqman primers (all from Applied Biosystems) for ICAM1 (Mm00516023_m1), claudin 1 (Mm00516701_m1), claudin 3 (Mm00515499_s1), claudin 5 (Mm00727012_s1), and ZO-1 (Mm00493699_m1). Real-time PCR was run for 35 cycles. Data were calculated using Δct, ΔΔct, and relative quantification ($2^{-\Delta\Delta CT}$).

Evans Blue Infusion. The 2% (wt/vol) Evans Blue (Sigma) was dissolved in PBS, filtered through a 45-μm filter (Millipore), and animals were infused i.v. with 200 μl 1 h before sacrifice, when mice were cardially perfused with 30 mL of PBS. Macroscopic images were taken using a Canon EOS 650 camera.

Dextran Infusion and Two-Photon Microscopy. A cranial window was implanted directly before two-photon microscopy imaging placed on the upper half of the cerebellum. Mice were anesthetized with ketamin (100 mg/kg) and xylazin (10 mg/kg) i.p. and placed on a head restrainer. Skin was removed from the skull, and a circular piece of bone was extracted using a drill, leaving the meninges untouched. The window was sealed with a round glass coverslip and surgical glue. Although still in anesthesia, mice were placed under the two-photon microscope, FITC-labeled dextran (20,000 kDa, Sigma) was dissolved at a concentration of 2 M in PBS, filtered through a 45-μm filter (Millipore), and animals were infused i.v. right before the first picture was taken. Mice were killed after the procedure. Statistical evaluation of two-photon images was done using imaris software (Bitplane). Mean fluorescence intensity values were measured of three spots per picture adjacent to the vessel boarder and related to fluorescence intensity inside the corresponding vessel.

Electron Microscopy. Transmission electron microscopy (TEM) was used to visualize ultrastructural changes in treated and untreated EAE mice compared with wild-type animals. Samples from the medulla oblongata, the cerebellum, and the cortex were prepared from each animal and fixed overnight using 2.5% (wt/vol) glutaraldehyde buffered in cacodylate buffer. The embedding procedure comprised fixation in 1% osmiun tetroxide, dehydration in a graded ethanol series intermingled by an incubation step with uranyl acetate [between the 50% and 90% (vol/vol) ethanol step], and finally rinsing in propylene oxide. The specimens were then embedded in epoxy resins that polymerized for 16 h at 60 °C. After embedding, first semithin sections (0.5 μm) were cut using an ultramicrotome (Leica Ultracut UCT) with a diamond knife. Sections were stained with Toluidine blue, placed on glass slides, and examined by light microscopy to select appropriate areas for ultrathin preparation. Ultrathin sections (50-70 nm) were cut again using an ultramicrotome. Sections were mounted on copper grids and contrasted with uranyl acetate for 2–3 h at 42 °C and lead citrate for 20 min at room temperature. These samples were imaged, and digital pictures were taken with an FEI Tecnai G2 Spirit Biotwin TEM at an operating voltage of 120 kV.

1. Bolstad BM, Irizarry RA, Astrand M, Speed TP (2003) A comparison of normalization methods for high density oligonucleotide array data based on variance and bias. *Bioinformatics* 19(2):185–193.
2. Sales G, Calura E, Martini P, Romualdi C (2013) Graphite Web: Web tool for gene set analysis exploiting pathway topology. *Nucleic Acids Res* 41(Web Server issue):W89–W97.
3. Schindelin J, et al. (2012) Fiji: An open-source platform for biological-image analysis. *Nat Methods* 9(7):676–682.

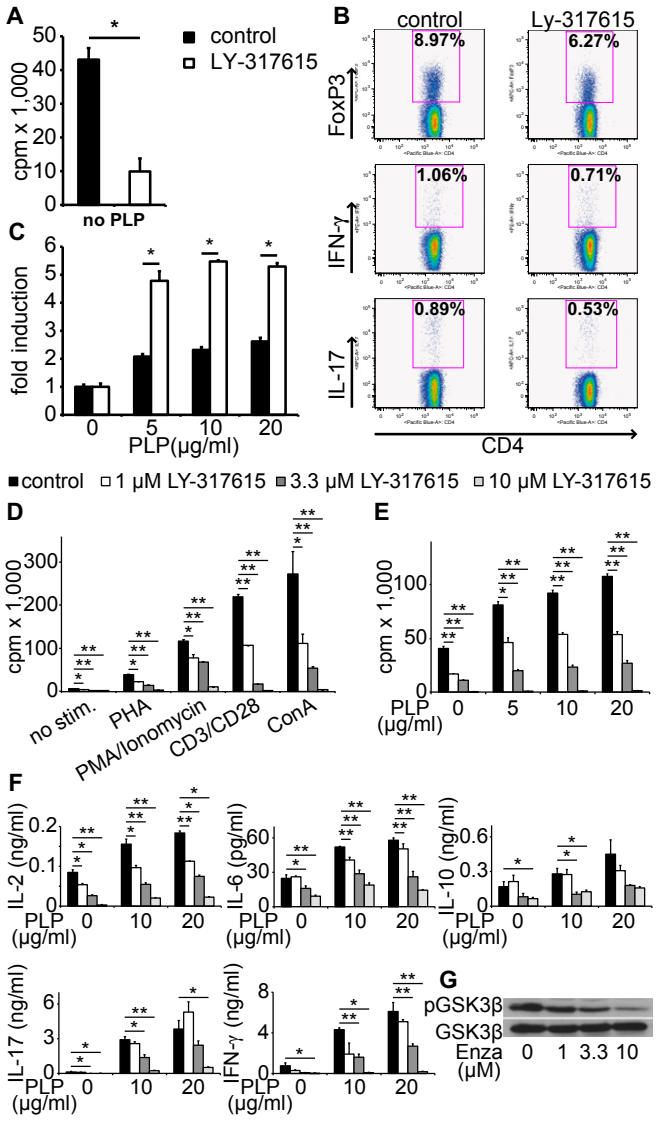

Fig. S1. LY-317615 inhibits EAE independent of T cells. (*A*) Proliferation of T cells from control- vs. LY-317615-treated SJL mice without stimulation. (*B*) Intracellular flow cytometry analysis of $CD4^+$ T cells from control- and LY-317615–treated SJL mice. Expression of FoxP3, IL-17, and IFN-γ are shown. (*C*) Antigen-specific proliferation of T cells from immunized SJL mice treated with control vs. LY-317615. Proliferation index is shown. (*A*–*C*) One representative experiment is shown of three independent experiments. $*P < 0.05$ according to Student *t* test. (*D*) T-cell proliferation triggered by the antigen-independent stimuli PHA, PMA/Ionomycin, CD3/CD28, and ConA. LY-317615 has been added in increasing concentrations. (*E*) Proliferation of lymph-node cells from immunized SJL mice, restimulated in vitro with ascending doses of $PLP_{139–151}$, similarly supplemented in vitro with increasing concentration of LY-317615. (*F*) T-cell cytokines IL-2, IL-6, IL-10, IL-17, and IFN-γ measured by ELISA from $PLP_{139–151}$-restimulated LN cells. (*G*) Western blot of GSK3β and phosphorylated GSK3β from PLP-restimulated LN cells.

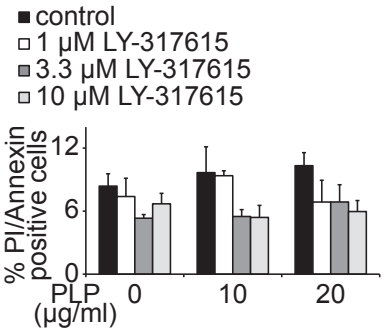

Fig. S2. LY-317615 doe not cause apoptosis in T cells. Flow cytometric analysis of T cells using Annexin/PI. Lymph-node cells were restimulated in vitro with $PLP_{139–151}$ and ascending doses of LY-317615 for the indicated time periods. PI/Annexin-positive populations are shown as percentages of CD4-positive cells. Data are means ± SD from two independent experiments.

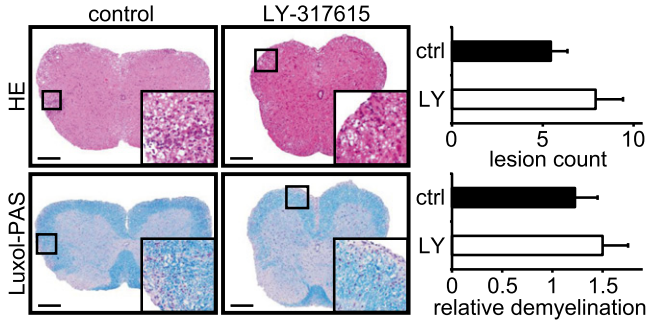

Fig. S3. Impact of LY-317615 on neuroinflammation in PT-EAE. H&E-stained (*Upper*) and Luxol-PAS–stained (*Lower*) slides of spinal cords from diseased C57BL/6 mice and their statistical evaluation. Representative slides are shown, and statistics were obtained from at least five mice per group. $*P < 0.05$ according to Student *t* test. (Scale bars: 200 μm.)

A

naive setup

index	pathway	p value	pathway genes	affected genes	status
1	NF-kappa B signaling pathway	0,01123	74	11	inhibited
2	Osteoclast differentiation	0,03385	110	13	inhibited
3	Cholinergic synapse	0,03491	93	11	inhibited
4	Glutamatergic synapse	0,03491	85	10	activated
5	Chagas disease (American trypanosomiasis)	0,04026	89	10	activated
6	Dopaminergic synapse	0,04286	115	12	inhibited
7	Vascular smooth muscle contraction	0,04471	106	11	inhibited

inflamed setup

index	pathway	p value	pathway genes	affected genes	status
1	NF-kappa B signaling pathway	0.00004	74	19	activated
2	Chronic myeloid leukemia	0.00028	71	17	inhibited
3	Renal cell carcinoma	0.00030	61	15	inhibited
4	Pancreatic cancer	0.00032	68	16	inhibited
5	Epstein-Barr virus infection	0.00370	80	16	inhibited
6	Prostate cancer	0.00370	87	17	inhibited
7	HIF-1 signaling pathway	0.00558	104	19	inhibited
8	***Leukocyte transendothelial migration***	***0.00678***	***86***	***16***	***inhibited***
9	Toll-like receptor signaling pathway	0.00678	93	17	activated
10	Herpes simplex infection	0.00820	102	18	activated
11	Influenza A	0.00931	104	18	activated
12	***TGF-beta signaling pathway***	***0.00931***	***83***	***15***	***inhibited***
13	Fc gamma R-mediated phagocytosis	0.01243	86	15	inhibited
14	Jak-STAT signaling pathway	0.01244	100	17	inhibited
15	Chagas disease (American trypanosomiasis)	0.01747	89	15	inhibited
16	Neurotrophin signaling pathway	0.01821	112	18	inhibited
17	Osteoclast differentiation	0.03118	110	17	inhibited
18	Measles	0.04131	98	15	activated
19	Cell cycle	0.04522	115	17	inhibited

Fig. S4. (Continued)

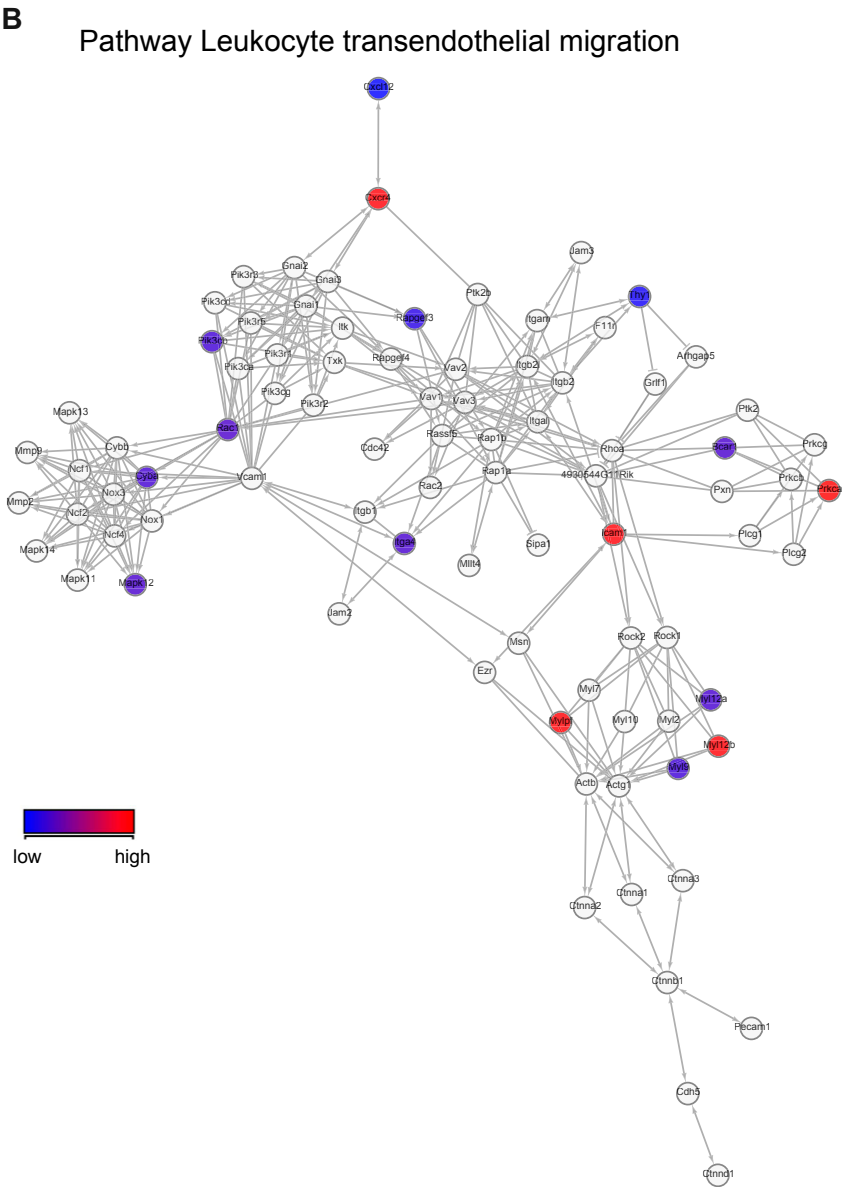

Fig. S4. (Continued)

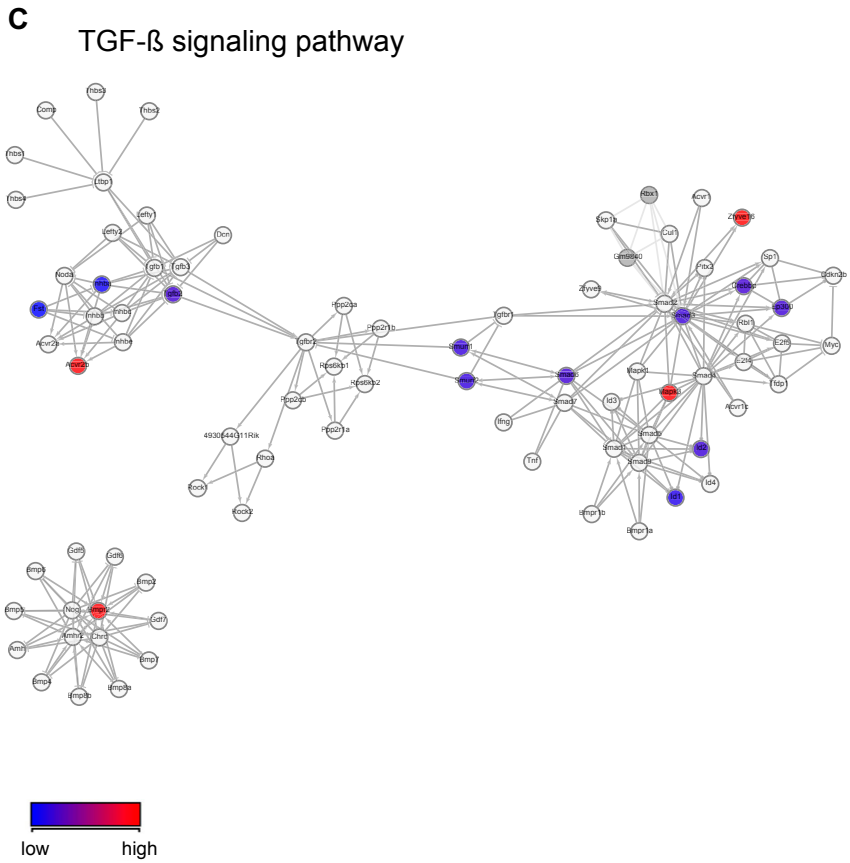

Fig. S4. Microarray mRNA expression analysis. MBMEC were cultured for 8 h in the presence of LY-317615 either in a naïve or an inflamed in vitro setting [containing TNF-α (500 U/mL) and IFN-γ (500 U/mL)]. Microarray was performed from three biological replicates of each sample. (*A*) Hypergeometric enrichment analysis of KEGG pathways among the differentially expressed genes (FDR < 0.05 and fold change > 1.2). (*B*) Pathway leukocyte transendothelial migration. (*C*) TGF-β signaling pathway. Red Genes are highly expressed, and blue genes are suppressed in LY-317615–treated MBMEC.

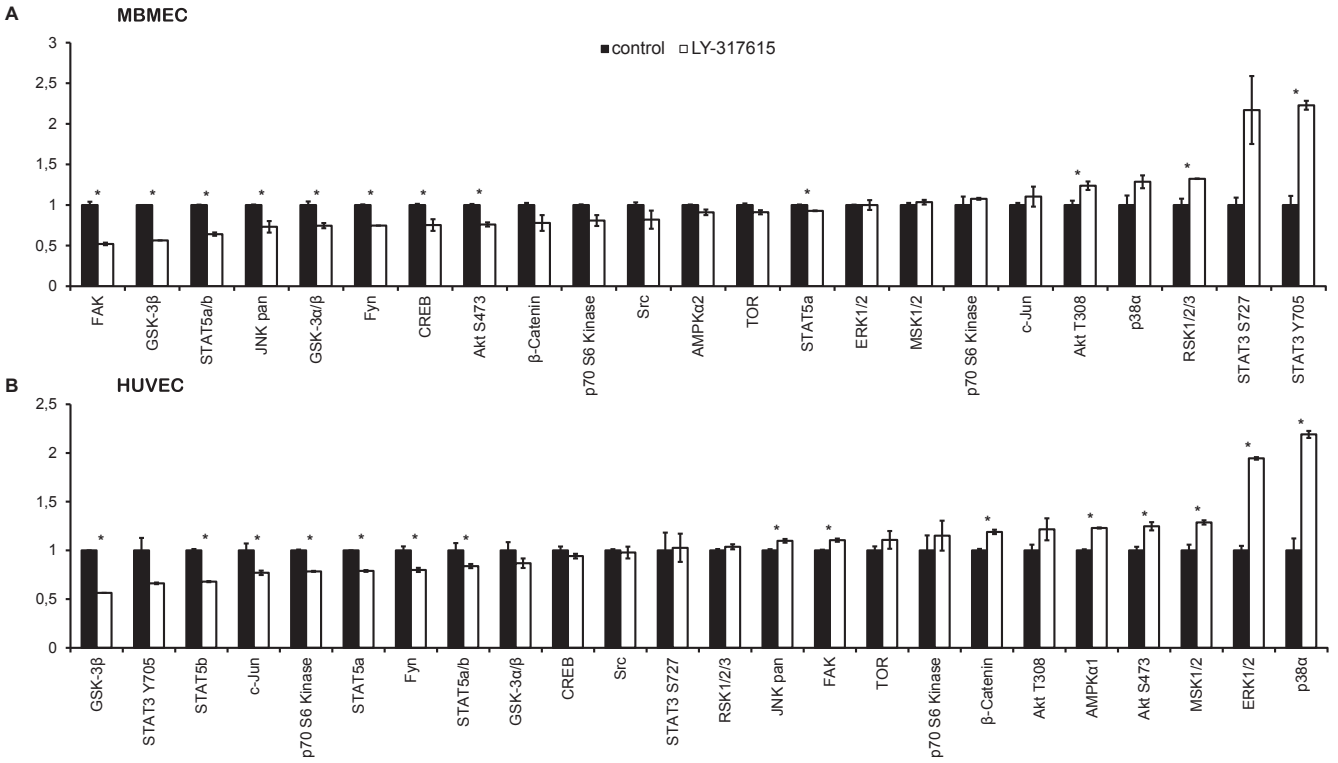

Fig. S5. Phospho-kinase antibody array. Cell lysates from (*A*) MBMEC and (*B*) HUVEC were tested on phosphorylation of 23 proteins. Mean ± SD from two replicates are shown. $*P < 0.05$ according to Student *t* test.

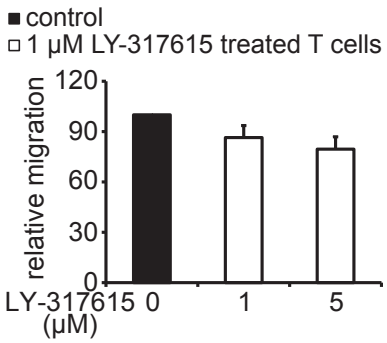

Fig. S6. Empty-field migration of T cells. T-cell migration through transwell without layer of endothelial cells as a control for the data shown in Fig. 3.